

# Extended High-gain Observer based Adaptive Control of Flexible-joint Surgical Robot \*

Shuizhong. Zou, Bo. Pan, Yili. Fu, and Shuxiang. Guo

**Abstract**—Due to the surgical robot flexible joint state vectors are not all measurable, in order to reduce the effect of the modeling errors and nonlinear factors of the flexible-joint manipulator caused by gravity and friction, an extended high-gain observer (EHGO) based adaptive control algorithm is designed to perform the position tracking control of the flexible-joint manipulator. First, gravity and friction are fed forward to reduce the nonlinearity of the robotic manipulator. Secondly, an extended high gain observer is used to observe the angular velocity of the joint and correct compensation errors of gravity and friction in real time. Finally, EHGO based adaptive controller is used to eliminate the inertia parameter measurement errors of the dynamic model, and to achieve high precision position tracking control. Simulation experiments show that the proposed control method can improve the position tracking accuracy of the flexible-joint manipulator and restrain the flexible-joint vibration obviously, and thus verifies that the designed controller can meet the requirements of accurate tracking control of the surgical robot.

Key Words: Surgical Robot, Adaptive control, Extended High Gain Observer, Flexible-joint manipulator Manipulator.

## I. INTRODUCTION

Flexible-joint have been widely used in surgical robots due to the lighter mass, less energy consumption, better maneuverability and safety. But the joint modeling errors, gravity, friction and other nonlinear factors make the precise control of flexible-joint manipulators more difficult. By the parameters identification of the joint dynamic model derived to obtain the accurate gravity and friction items, the precise compensation of gravity and friction can effectively reduce the nonlinear effects of the flexible-joint. In addition, since the flexible-joint is essentially a kind of under-actuated nonlinear system, and not all state variables can be measured, it is a good choice to observe all the state variables of the joint by the observer. Luenberger observer is a most commonly used linear observer[1, 2], which is not robust to the uncertainties of the model and quantization noises. The methods based Kalman filter[3, 4] need to know the noise variance information assumed as Gauss noise. Nonlinear observer[5-7] is robust to the uncertainties of the model, but it is often sensitive to the measurement noises, which will limit nonlinear observer to be used in practical applications. High gain observer[6, 8-10] is a nonlinear observer proposed by H.k.khalil and F.Esfandiari in 1992, with quick convergence

and simple adjustments of gain matrix, which has been widely used in the practical applications due to the good observation performances.

Due to the joint nonlinearity and modeling errors, the researchers have been carried out many studies on the control of flexible-joint manipulator. These developed control methods of the flexible-joint manipulator mainly includes: linearization technique[11], pseudo linearization of state space, nonlinear compensation of dynamic feedback, optimal control and singular perturbation control[12, 13], etc.. In practical applications, due to the influence of the uncertain factors such as parameter perturbations and load disturbances, it is difficult to obtain the accurate dynamics of the flexible-joint manipulator, therefore, the adaptive control[14-16] of the flexible-joint manipulator with uncertain factors has become a hot topic in the current research.

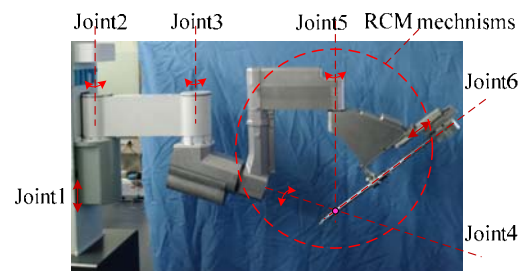


Figure 1 The celiac minimally invasive surgical robot systems

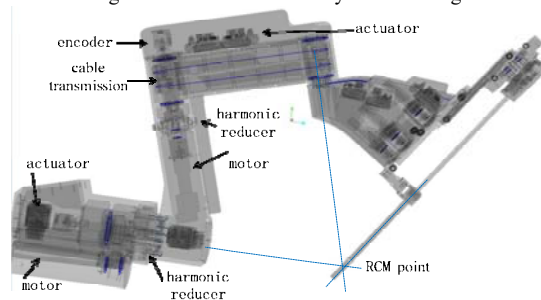


Figure 2 Slave manipulator and RCM mechanisms

The research background of this paper is the celiac minimally invasive surgical robot independently developed by Harbin Institute of Technology, as shown in figure 1, the developed celiac minimally invasive surgical robot systems include two parts: the position adjustment mechanisms and the remote center motions mechanisms (RCMM). The position adjustment mechanisms locate the incisions in the patient's body surface, which are made up of three passive joints, including the first prismatic joint, second revolute joint and third revolute joint. RCMM implement the position and pose adjustment of surgical instruments within the patient's body, which composed of three active joints, including the fourth

\* This work was supported by the National High Technology Research and Development Program of China ("863 Program") (Grant No. 2012AA041601), the National Natural Science Foundation of China (Grant No.61305139), Self-Planned Task (No. SKLRS201406B) of State Key Laboratory of Robotics and System (HIT)

revolute joint, fifth revolute joint, sixth prismatic joint. As shown in figure 2, each of the flexible joint of RCMM is composed of motor, position encoder by motor side, harmonic reducer, cable transmission, position encoder by link side.

The structure of this paper are as follows: the first part is the modeling and parameter linearization of the flexible joint of RCMM. The second part is the design of EHGO to estimate the angular velocity and disturbance torque of the flexible joint of RCMM in real time. The third part is the design of adaptive controller based on EHGO for the position tracking control of the flexible joint of RCMM. The fourth part is the angular velocity and disturbance torque estimation experiments of EHGO, and the position tracking experiments of the adaptive controller based on EHGO.

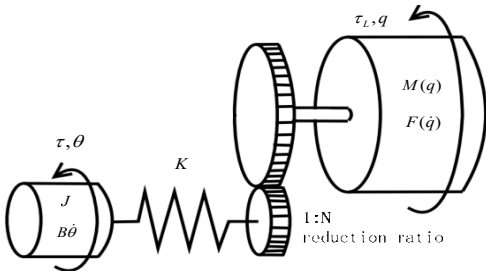


Figure 3 The elastic structure of the joint of RCMM

## II. MATERIALS AND METHODS

### A. Dynamic modeling and parameters linearization of RCMM

As shown in figure 3, by applying Bridges and Dawson model[17] and using the Euler-Lagrange method, the dynamic model of RCMM can be derived as:

$$\begin{cases} M(q)\ddot{q} + C(q, \dot{q})\dot{q} + G(q) + F(\dot{q}) = K(N^{-1}\theta - q) \\ J\ddot{\theta} + B\dot{\theta} + N^{-1}K(N^{-1}\theta - q) = \tau \end{cases} \quad (1)$$

where,  $q = [q_1, q_2, d_3]^T$ ,  $q, \dot{q}, \ddot{q} \in R^3$  and  $\theta = [\theta_1, \theta_2, \theta_3]^T$ ,  $\theta, \dot{\theta}, \ddot{\theta} \in R^3$  denote the vector of the angular position, angular velocity and angular acceleration of links and motors, respectively,  $M(q) \in R^{3 \times 3}$ ,  $J \in R^3$  are the inertia matrices of links and motors, respectively,  $C(q, \dot{q}) \in R^{3 \times 3}$  denotes the centripetal-coriolis matrix of links,  $B, K, N \in R^{3 \times 3}$  are the positive-definite constant diagonal matrices representing motor damping, joint linear stiffness and gear reduction ratio of each reducer, respectively,  $G(q), F(\dot{q}) \in R^3$  indicate the gravity vector and friction vector of links, respectively,  $\tau \in R^3$  is the output torque vector of motor, For simplification,  $M(q)$  is written as  $M$ ,  $C(q, \dot{q})$  is written as  $C$ ,  $G(q)$  is written as  $G$ .

Since Stribeck model can cover coulomb, viscous and Stribeck friction, especially when  $\delta_s = 1$ , the model is suitable for industrial control. In this paper, the friction model is defined as:

$$\begin{cases} F(\dot{q}) = [F_1(\dot{q}_1), F_2(\dot{q}_2), F_3(\dot{q}_3)]^T \\ F_i(\dot{q}_i) = (f_{i1} + f_{i2}e^{-f_{i4}|\dot{q}_i|}) \text{sgn}(\dot{q}_i) + f_{i3}\dot{q}_i, i=1,2,3 \end{cases} \quad (2)$$

where,  $f_{i1}, \dots, f_{i4}$  denote the  $i$ th joint's coulomb coefficient, additional stiction force coefficient, Stribeck effect coefficient, and viscous coefficient, respectively.

In order to facilitate the parameter identification of the dynamic model of RCMM, the formula (1) should first be linearized as:

$$\tau = Y(\Theta, \dot{\Theta}, \ddot{\Theta})\pi \quad (3)$$

where,  $\Theta = [\theta, q]^T$  denotes joint position vector,

$\pi = [\pi_d, \pi_g, \pi_f]^T$  denote the vector of unknown

parameters,  $Y(\Theta, \dot{\Theta}, \ddot{\Theta}) = [Y_d[3 \times 4] \quad Y_g[3 \times 3] \quad Y_f[3 \times 5]]$  is a regression matrix, and the detail of  $Y, \pi$  are shown in the appendix.

By the gravity and friction compensation and its error correction by EHGO, adaptive controller don't need considering the effect of gravity and friction. In order to facilitate the design of adaptive controller, the formula (1) can also be linearized as:

$$\begin{cases} M(q)\ddot{q} + C(q, \dot{q})\dot{q} = \tau_s = Y_s(q, \dot{q}, \ddot{q})\pi_d \\ \tau_s = K(N^{-1}\theta - q) - G(q) - F(\dot{q}) \end{cases} \quad (4)$$

where,  $q, \dot{q}, \ddot{q}$  denote the vector of the angular position, angular velocity and angular acceleration of links,  $Y_s$  is a corresponding regression matrix,  $\pi_d$  is the dynamic model inertia parameters.

### B. EHGO design

Let us define some state vectors as follows:

$$u = \tau = [\tau_1, \tau_2, \tau_3]^T, \mathbf{x}_1 = [q_1, q_2, d_3]^T, \mathbf{x}_2 = \dot{\mathbf{x}}_1, \mathbf{x}_3 = [\theta_1, \theta_2, \theta_3]^T, \mathbf{x}_4 = \dot{\mathbf{x}}_3, \mathbf{x} = [\mathbf{x}_1, \mathbf{x}_2, \mathbf{x}_3, \mathbf{x}_4]^T,$$

By formula (1), the state space equation of RCMM can be expressed as:

$$\dot{\mathbf{x}} = \begin{bmatrix} \mathbf{x}_2 \\ \phi_1(\mathbf{x}) \\ \mathbf{x}_4 \\ \phi_2(\tau, \sigma, \mathbf{x}) \end{bmatrix}, \mathbf{y} = \begin{bmatrix} \mathbf{y}_1 \\ \mathbf{y}_2 \end{bmatrix} = \begin{bmatrix} \mathbf{x}_1 + \Delta\mathbf{x}_1 \\ \mathbf{x}_2 + \Delta\mathbf{x}_2 \end{bmatrix} \quad (5)$$

where,  $\Delta\mathbf{x}_1, \Delta\mathbf{x}_2$  denote the measurement noise of motor side encoders and link side encoders, respectively,  $\sigma$  indicates the disturbance torque caused by the dynamic modeling error,

$$\phi_1(\mathbf{x}) = M^{-1} \left( K(N^{-1}\mathbf{x}_3 - \mathbf{x}_1) - C(\mathbf{x}_1, \mathbf{x}_2)\mathbf{x}_2 - F(\mathbf{x}_2) \right),$$

$$\phi_2(\tau, \Delta\tau, \mathbf{x}) = J^{-1} \left( \tau + \sigma - B\mathbf{x}_4 - N^{-1}K(N^{-1}\mathbf{x}_3 - \mathbf{x}_1) \right).$$

By the formula (4), an EHGO can be designed as follows:

$$\begin{cases} \dot{\hat{\mathbf{x}}}_1 = \hat{\mathbf{x}}_2 + \frac{\alpha_1}{\varepsilon}(\mathbf{y}_1 - \hat{\mathbf{x}}_1) \\ \dot{\hat{\mathbf{x}}}_2 = \phi_1(\mathbf{x}) + \frac{\alpha_2}{\varepsilon^2}(\mathbf{y}_1 - \hat{\mathbf{x}}_1) \\ \dot{\hat{\mathbf{x}}}_3 = \hat{\mathbf{x}}_4 + \frac{\beta_1}{\varepsilon}(\mathbf{y}_2 - \hat{\mathbf{x}}_2) \\ \dot{\hat{\mathbf{x}}}_4 = \phi_2(\tau, \sigma, \mathbf{x}) + \frac{\beta_2}{\varepsilon^2}(\mathbf{y}_2 - \hat{\mathbf{x}}_2) \\ \dot{\hat{\sigma}} = \frac{\beta_3}{\varepsilon^3}(\mathbf{y}_2 - \hat{\mathbf{x}}_2) \end{cases} \quad (6)$$

where,  $\dot{\hat{\sigma}}, \hat{\mathbf{x}}_1, \hat{\mathbf{x}}_i, (i=1, 2, 3)$  denote the observer values of  $\dot{\sigma}, \mathbf{x}_1, \dot{\mathbf{x}}_i, \varepsilon > 0$  is a small parameter, the observer constants  $\alpha_1, \alpha_2, \beta_1, \beta_2, \beta_3$  are chosen such that the polynomial  $s^2 + \alpha_1s + \alpha_2$  and  $s^3 + \beta_1s^2 + \beta_2s + \beta_3$  are Hurwitz, such as  $\alpha_1 = 3, \alpha_2 = 2, \beta_1 = 6, \beta_2 = 11, \beta_3 = 6$ .

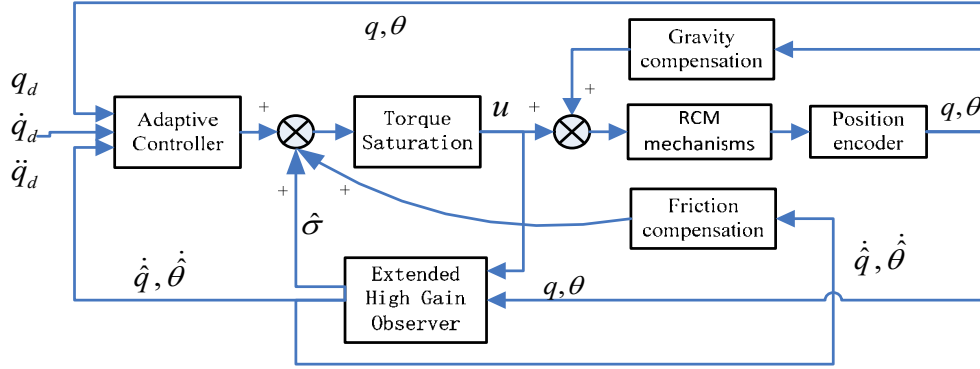


Figure 4 Adaptive control for RCM mechanisms

### C. EHGO based on Adaptive controller design

Define the following expressions as:

$$e = q - q_d, \dot{q}_r = \dot{q}_d - \lambda e, r = \dot{q} - \dot{q}_r = \dot{e} + \lambda e,$$

$$\theta_d = N\dot{q}_d, e_s = \theta - \theta_d$$

where,  $\theta, \theta_d, q, q_d$  denote the vectors of motor actual position, motor desired position, link actual position and the link desired position, respectively,  $N$  is a gear reduction ratio matrix,  $e, e_s$  indicate the error vector between the desired position and the actual position of link and motor, respectively.

In figure 4, with the gravity and friction compensation and its error correction item  $\hat{\sigma}$  by EHGO, adaptive controller don't need considering the effect of gravity and friction, at the same time, only the estimated values of the inertia parameters must be known, from the formula (1), (4), the adaptive controller can be designed as follows:

$$\begin{aligned} \tau = N^{-1} \left( \hat{M}(q)\ddot{q}_r + \hat{C}(q, \dot{q})\dot{q}_r - K_d r \right) \\ + NJ\ddot{q}_d - K_v(\dot{\theta} - N\dot{q}) \end{aligned} \quad (7)$$

$$\dot{\hat{\pi}}_d = -\Gamma Y_S^T(q, \dot{q}, \dot{q}_r, \ddot{q}_r)r \quad (8)$$

$$J\ddot{e}_s + K_v\dot{e}_s = 0 \quad (9)$$

where,  $\Gamma$  is a positive definite symmetric matrix,  $\hat{M}, \hat{C}$  are the link estimated inertia matrix, centripetal-coriolis matrix,  $Y_S^T$  is a corresponding regression matrix,  $\hat{\pi}_d$  is the estimated inertia parameters of the dynamic model,  $K_v, K_d$  is positive definite diagonal matrix,  $K_v$  is a control gain to suppress vibration of the flexible joint, and  $K_d$  is the control gain to eliminate the link position tracking error, Moreover, the formula (7), (8), (9) are the control law of adaptive controller, the adaptation law, and the boundary layer condition, Since  $J, K_v$  are positive definite diagonal matrix, the boundary layer system (9) is asymptotically stable and convergent.

Lyapunov function is chosen as:

$$V(t) = \frac{1}{2}r^T M r + \frac{1}{2}\hat{\pi}_d^T \Gamma \hat{\pi}_d \quad (10)$$

Since  $M, \Gamma$  are positive definite symmetric matrices, it can be known that  $V(t) \geq 0$ .

The differential of the formula (15) can be obtained as:

$$\begin{aligned}
\dot{V}(t) &= r^T M \dot{r} + \frac{1}{2} r^T \dot{M} r + \tilde{\pi}_d^T \Gamma \dot{\tilde{\pi}}_d \\
&= r^T (M \dot{r} + Cr) + \frac{1}{2} r^T (\dot{M} - 2C) r + \tilde{\pi}_d^T \Gamma \dot{\tilde{\pi}}_d \\
&= r^T (-K_d r - N(J\ddot{e}_s + K_v \dot{e}_s) + Y_s \tilde{\pi}_d) + \tilde{\pi}_d^T \Gamma \dot{\tilde{\pi}}_d \\
&= -r^T K_d r + \tilde{\pi}_d^T (Y_s^T r + \Gamma \dot{\tilde{\pi}}_d) \\
&= -r^T K_d r \leq 0
\end{aligned} \tag{11}$$

By formula (11), it can be yielded that the adaptive controller expressed by formula (7) is globally stable.

### I. IMPLEMENTATION AND EXPERIMENTAL RESULT H

Compared to the first and second joint, the mass of the third joint of RCMM is relatively small, which causes too small coupling effects to ignore its coupling influence on the other joints. In order to demonstrate the performances of extended high gain observer, the estimation of the velocities and disturbance torque of the first two joints of RCMM are performed by EHGO. By the parameters identification, the dynamic parameters of the first two joints of RCMM are given as:

$$\begin{aligned}
J_1 &= 1.42e - 5 \text{kg.m}^2, J_2 = 1.05e - 6 \text{kg.m}^2, \\
m_1 &= 5.92 \text{kg.m}^2, m_2 = 2.22 \text{kg.m}^2, \\
N_1 &= 360, N_2 = 320, B_1 = 3.72e-5, B_2 = 1.37e-5, \\
K_1 &= 160 \text{N.m / rad}, K_2 = 100 \text{N.m / rad}, \\
F_1(\dot{q}_1) &= (13.04 + 1.05e^{-24.6|\dot{q}_1|}) \text{sgn}(\dot{q}_1) + 12.79\dot{q}_1, \\
F_2(\dot{q}_2) &= (1.66 + 0.39e^{-35|\dot{q}_2|}) \text{sgn}(\dot{q}_2) + 0.88\dot{q}_2, \\
\varepsilon &= 0.06, \alpha_1 = 3, \alpha_2 = 2, \beta_1 = 6, \beta_2 = 11, \beta_3 = 6, \\
\tau_1 &= 3.6 \sin\left(\frac{\pi}{6} t\right), \tau_2 = 3.2 \sin\left(\frac{\pi}{3} t\right).
\end{aligned}$$

As shown in Figure 5, 6, 8, 9, there are the certain deviation between the desired values and estimated values of position and velocity of links at the start moment, but the differences between these estimates values and actual values are almost converge to zero over the subsequent time. Figure 7, 10 show that the error of the estimated disturbance torques in joints are relatively small at the initial time but quickly converge to their desired values.

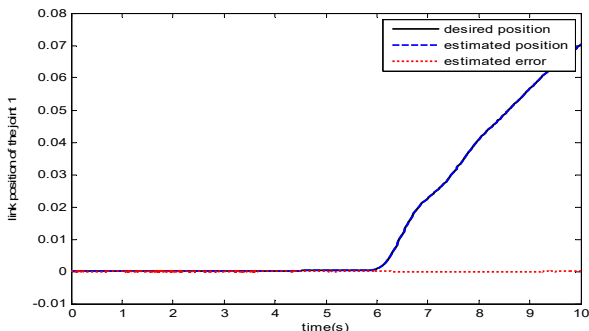


Figure 5 The link position estimation of the first joint of RCMM

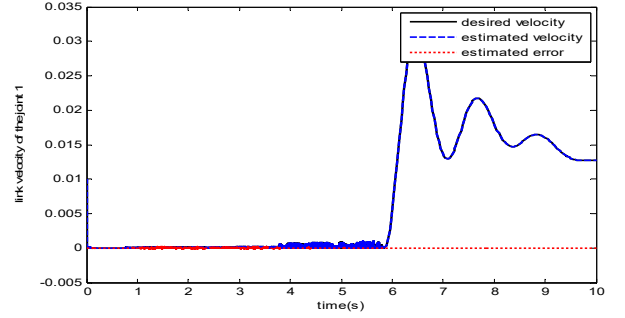


Figure 6 The link velocity estimation of the first joint of RCMM

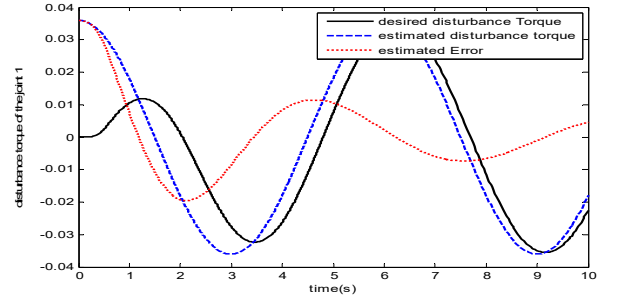


Figure 7 The disturbance torque estimation of the first joint of RCMM

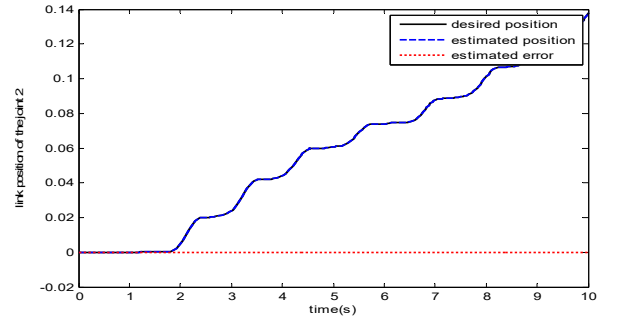


Figure 8 The link position estimation of the second joint of RCMM

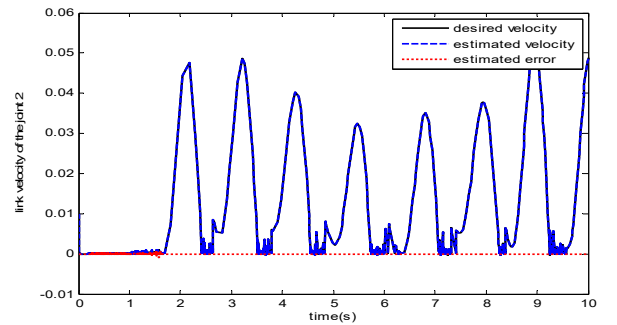


Figure 9 The link velocity estimation of the second joint of RCMM

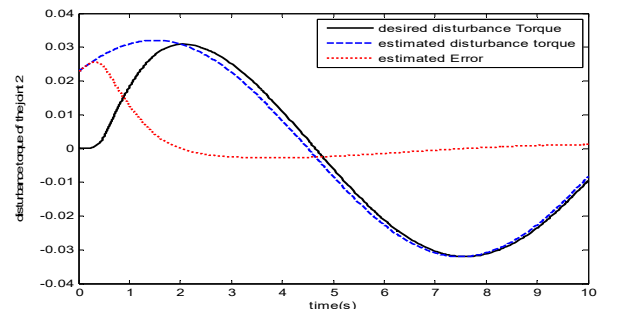


Figure 10 The disturbance torque estimation of the second joint of RCMM

In order to demonstrate the trajectory tracking control performances of the adaptive controller, the position tracking control experiments of the first two joints of RCMM are performed. The adaptive controller parameters are given as:

$$\hat{\Lambda} = \begin{bmatrix} 5 & 0 \\ 0 & 5 \end{bmatrix}, K_d = \begin{bmatrix} 100 & 0 \\ 0 & 100 \end{bmatrix}, K_v = \begin{bmatrix} 10 & 0 \\ 0 & 10 \end{bmatrix}, \Gamma = \begin{bmatrix} 1 & 0 & 0 & 0 \\ 0 & 1 & 0 & 0 \\ 0 & 0 & 1 & 0 \\ 0 & 0 & 0 & 1 \end{bmatrix},$$

$$q_{d1} = \sin\left(\frac{\pi}{3}t\right), q_{d2} = \sin\left(\frac{\pi}{3}t\right)$$

The dynamic parameter element  $\pi_d$  and the regression matrix element  $Y_d$  are described in detail in the appendix.

As shown in Figure 11, 12, 13, 14, there are the certain deviation between the desired values(position, velocity) and the tracking values(position, velocity) at the initial time but these differences quickly converge to zero. Moreover, in order to guarantee the stability of the whole system, the gains of the controller should meet the conditions:  $K_d \gg K_v > 0$ .

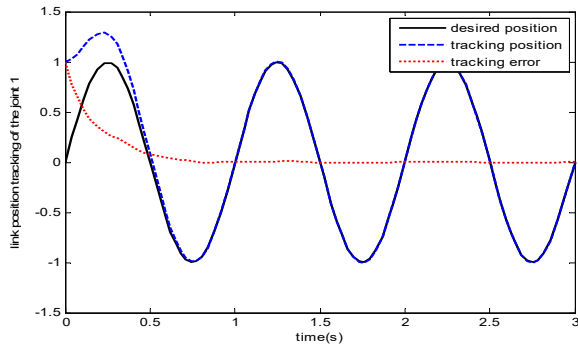


Figure 11 The link position tracking of the joint 1 of RCMM

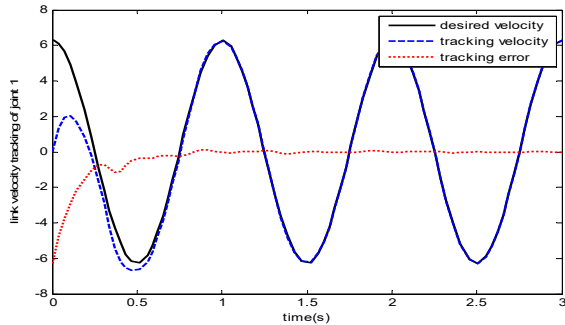


Figure 12 The link velocity tracking of the joint 1 of RCMM

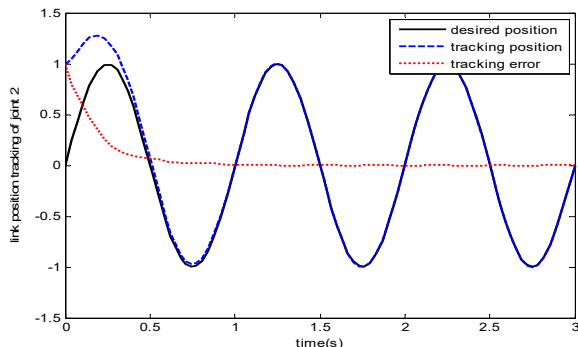


Figure 13 The link position tracking of the joint 2 of RCMM

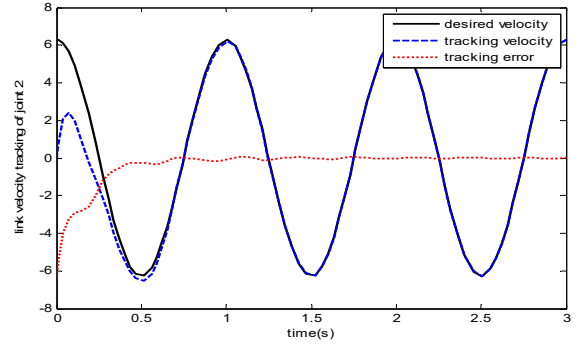


Figure 14 The link velocity tracking of the joint 2 of RCMM

## II. CONCLUSION

In this paper, by the parameters identification of the joint dynamic model derived to obtain the accurate gravity and friction items, the feedforward compensation of gravity and friction to reduce the nonlinearities of the joint are carried out, and then an EHGO is designed to in real-time estimate the joint velocities and disturbing torques caused by not fully accurate compensation of gravity and friction, which also improve the accuracy of the dynamic modeling. Finally, the control of position tracking and vibration inhibition of the first joint of RCMM by an adaptive controller are performed. The controller proposed in this paper does not require an acceleration signal, and the adaptive law only needs to update the inertial parameters, which greatly improve the controller performances for the position trajectory tracking and vibration suppression of the flexible joint of RCMM. Simulation experiments show that the proposed controller fully meet the real-time control requirements of the RCMM of the surgical robot, meanwhile, the proposed controller also adapted to the position tracking and vibration suppression control requirements of the other kind of robot with flexible-joint manipulator.

## APPENDIX

According to the three joint axes of RCMM intersecting at a point O (the remote centre point), the point O is set as the origin of all coordinate systems of RCMM (see Figure 10). The coordinate system  $\{0\}$  is the base coordinate system, and its Z axis is perpendicular to the paper-based inward. According to the D-H algorithm, the X axis direction of the coordinate systems  $\{1\}$ ,  $\{2\}$ ,  $\{3\}$  are perpendicular to the paper-based inward.

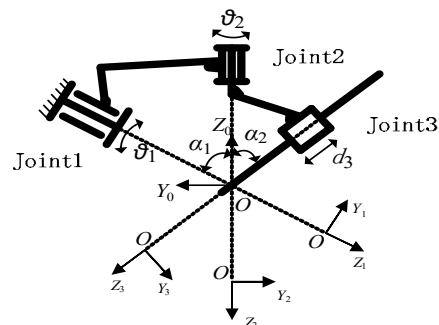


Figure 14 the layout of the coordinate systems of RCMM

Joint	$\alpha_i/^\circ$	$l_i/\text{mm}$	$d_i/\text{mm}$	$q_i/^\circ$
1	106	0	0	$q_1$
2	74	0	0	$q_2$
3	51	0	$d_3$	0

Table 7 D-H parameter table of RCMM

According to the coordinate systems of RCMM, the D-H parameter table can be obtained as shown in Table 7. Using the Lagrange-Euler algorithm, the complete dynamic equation of RCMM can be derived as:

$$\begin{cases} M(q)\ddot{q} + C(q, \dot{q})\dot{q} + G(q) + F(\dot{q}) = K(N^{-1}\theta - q) \\ J\ddot{\theta} + B\dot{\theta} + KN^{-1}(N^{-1}\theta - q) = \tau \end{cases} \quad (12)$$

Formula (11) can be parametric linearization as

$$\tau = \mathbf{Y}(\Theta, \dot{\Theta}, \ddot{\Theta})\boldsymbol{\pi}$$

$$\mathbf{Y} = [Y_{d[3 \times 4]}, Y_{g[3 \times 3]}, Y_{f[3 \times 9]}],$$

$$\boldsymbol{\pi} = [\pi_d, \pi_g, \pi_f]^T, \pi_d = [\pi_{d1}, \dots, \pi_{d4}]^T,$$

$$\pi_g = [\pi_{g1}, \pi_{g2}, \pi_{g3}]^T, \pi_f = [\pi_{f1}, \pi_{f2}, \pi_{f3}]^T,$$

$$\pi_{f_i} = [f_{i0}, f_{i1}, f_{i2}, \beta_i, B_i]^T, i = 1, 2, 3.$$

The detailed expressions of the parameter  $\boldsymbol{\pi}$  are as follows:

$$[\pi_{g1}, \pi_{g2}, \pi_{g3}]^T = [-20.33, 0.34, 2.2]^T,$$

$$[f_{11}, f_{12}, f_{13}, f_{14}, B_1] = [13.04, 0.75, 12.78, 24.6, 3.73e-5],$$

$$[f_{21}, f_{22}, f_{23}, f_{24}, B_2] = [1.66, 0.39, 0.88, 35, 1.37e-5],$$

$$[f_{31}, f_{32}, f_{33}, f_{34}, B_3] = [0.001, 0.001, 0.256, 0.202, 3.23e-6],$$

$$[\pi_{d1}, \pi_{d2}, \pi_{d3}, \pi_{d4}]^T = [2.093, -1.362, 2.336, 3.085]^T$$

$$Y_{11} = 0.076\ddot{q}_1 + 0.276\ddot{q}_2,$$

$$Y_{12} = 0.924c_2^2\ddot{q}_1 - 1.848c_2s_2\dot{q}_1\dot{q}_2,$$

$$Y_{13} = 0.53c_2\ddot{q}_1 + 0.961c_2\ddot{q}_2 - 0.53s_2\dot{q}_1\dot{q}_2 - 0.961s_2\dot{q}_2^2,$$

$$Y_{14} = \dot{q}_1, Y_{15} = s_1, Y_{16} = -(9.42c_1s_2 + 2.6c_2s_1),$$

$$Y_{21} = 0.276\ddot{q}_1 + \ddot{q}_2, Y_{22} = 0.924c_2s_2\dot{q}_1^2 + \dot{q}_1,$$

$$Y_{23} = 0.961c_2\ddot{q}_1 + 0.265s_2\dot{q}_1^2, Y_{24} = \ddot{q}_2,$$

$$Y_{25} = 2.6(1 - c_1)s_2 - 9.42c_2s_1,$$

$$Y_{26} = (7.32c_2s_1 + 2.018(c_1 - 1)s_2)(d_3 - 0.63),$$

$$Y_{31} = \dots = Y_{35} = 0,$$

$$Y_{36} = \ddot{d}_3 + 2.02c_2 - 5.7c_1 - 0.47 - 2.02c_1c_2 + 7.32s_1s_2.$$

In the above expressions,  $c_1, c_2, s_1, s_2$  denote  $\cos(q_1), \cos(q_2), \sin(q_1), \sin(q_2)$ , respectively.

where  $c_1, c_2, s_1, s_2$  represent the shorthand notations for  $\cos(q_1), \cos(q_2), \sin(q_1), \sin(q_2)$ .

### References:

- [1]. Lorenz, R.D. and K.W. Van Patten, High-resolution velocity estimation for all-digital, ac servo drives. *Industry Applications, IEEE Transactions on*, 1991. 27(4): p. 701-705.
- [2]. Yang, S. and S. Ke, Performance evaluation of a velocity observer for accurate velocity estimation of servo motor drives. *Industry Applications, IEEE Transactions on*, 2000. 36(1): p. 98-104.
- [3]. Belanger, P.R., et al., Estimation of angular velocity and acceleration from shaft-encoder measurements. *The International Journal of Robotics Research*, 1998. 17(11): p. 1225-1233.
- [4]. Kim, H. and S. Sul, A new motor speed estimator using Kalman filter in low-speed range. *Industrial Electronics, IEEE Transactions on*, 1996. 43(4): p. 498-504.
- [5]. Talole, S.E., J.P. Kolhe and S.B. Phadke, Extended-state-observer-based control of flexible-joint system with experimental validation. *Industrial Electronics, IEEE Transactions on*, 2010. 57(4): p. 1411-1419.
- [6]. Ball, A.A. and H.K. Khalil, Analysis of a nonlinear high-gain observer in the presence of measurement noise. in *American Control Conference (ACC)*, 2011. 2011: IEEE.
- [7]. Zhang, Q., Adaptive observer for MIMO linear time varying systems. 2001.
- [8]. Nicosia, S. and A. Tornambè, High-gain observers in the state and parameter estimation of robots having elastic joints. *Systems & control letters*, 1989. 13(4): p. 331-337.
- [9]. Khalil, H.K. High-gain observers in nonlinear feedback control. in *Control, Automation and Systems*, 2008. ICCAS 2008. International Conference on. 2008: IEEE.
- [10]. Lee, K.W. and H.K. Khalil, Adaptive output feedback control of robot manipulators using high-gain observer. *International Journal of Control*, 1997. 67(6): p. 869-886.
- [11]. De Luca, A. and P. Lucibello, A general algorithm for dynamic feedback linearization of robots with elastic joints. in *Robotics and Automation*, 1998. Proceedings. 1998 IEEE International Conference on. 1998: IEEE.
- [12]. Spong, M.W., K. Khorasani and P.V. Kokotovic, An integral manifold approach to the feedback control of flexible-joint manipulator robots. *Robotics and Automation, IEEE Journal of*, 1987. 3(4): p. 291-300.
- [13]. Subudhi, B. and A.S. Morris, Singular perturbation approach to trajectory tracking of flexible robot with joint elasticity. *International Journal of Systems Science*, 2003. 34(3): p. 167-179.
- [14]. Spong, M.W., Adaptive control of flexible-joint manipulator manipulators. *Systems & Control Letters*, 1989. 13(1): p. 15-21.
- [15]. Ulrich, S. and J.Z. Sasiadek, On the Simple Adaptive Control of Flexible-Joint Space Manipulators with Uncertainties, in *Aerospace Robotics II*. 2015, Springer. p. 13-23.
- [16]. Ulrich, S., J.Z. Sasiadek and I. Barkana, Modeling and direct adaptive control of a flexible-joint manipulator. *Journal of Guidance, Control, and Dynamics*, 2012. 35(1): p. 25-39.
- [17]. Bridges, M.M. and D.M. Dawson, Redesign of robust controllers for rigid-link flexible-joint robotic manipulators actuated with harmonic drive gearing. *IEE Proceedings-Control Theory and Applications*, 1995. 142(5): p. 508-514.